Undergraduate Research Paper - Fall 2023

CubeSat Science Mission - Building a Radiometer

Luke Strachan, lstracha@nd.edu
Isaac Brej, ibrej@nd.edu
Advisor: Professor Jonathan Chisum, jchisum@nd.edu

IrishSat
University of Notre Dame
216 Stinson Remick Hall, Notre Dame, IN, 46556
irishsat@nd.edu

General Overview

The primary objective of the following undergraduate research was to design and characterize a radiometer for interfacing with Dr. Chisum's phased array-fed lens (PAFL) antennas within the context of the IrishSat's Cubesat project, CLOVER-Sat. The ultimate purpose of this work is to create a technological demonstration of novel millimeter-wave technology in low Earth orbit, showcasing the antenna's beamforming capabilities while operating efficiently through minimized power and volume in the satellite bus.

PAFL enhances traditional millimeter-wave technologies, such as lens antennas and phased array antennas (PAA), by leveraging the advantages of each while minimizing the associated disadvantages. Switched beach gradient index lens antennas exhibit poor performance due to fixed beam angles and the presence of nulls in the radiation pattern. Additionally, they require a specific focal length/diameter ratio of 0.5 for focusing. Phased array antenna spacing constraints necessary for proper beamforming consume large amounts of power and are expensive due to component costs.

PAFL operates by using a gradient index lens made of low-loss alumina material over a phased array and an optimization algorithm for superimposing multiple beams into a desired main beam at an arbitrary angle with diminished sidelobes. Additionally, spacing the antenna elements by 0.7λ instead of 0.5λ helps avoid the usual grading lobes resulting from antenna aliasing. By using multiple elements weighted by both phase and magnitude, this error can be corrected. By spacing elements in the array, heat dissipation is increased, thereby extending the operational time of the antenna, as overheating is less of a concern. Preliminary research suggests that the traditional PAA configuration consumes about $2.4W/cm^2$ of power, whereas the PAFL configuration proposed by Dr. Chisum and his research group consumes about $0.3W/cm^2$. Cost is minimized by using fewer integrated circuits (ICs) in the circuitry that drives the operation of the PAFL antenna, demonstrating about a 50% reduction in the number of ICs required for a 2D array to achieve similar performance compared to the PAA configuration [1]. Additionally, the static nature of the lens setup and a simple linear actuator allow for low-risk deployment when compared to reflector antennas. Figure 1 shows the current design for deploying PAFL.

The PAFL configuration presents five advantageous features that either match or improve upon current technology capabilities:

1. Low power and low heat dissipation
2. Low cost
3. Low-risk deployment
4. Ultra-wideband
5. Capable of being put on small payloads like a CubeSat

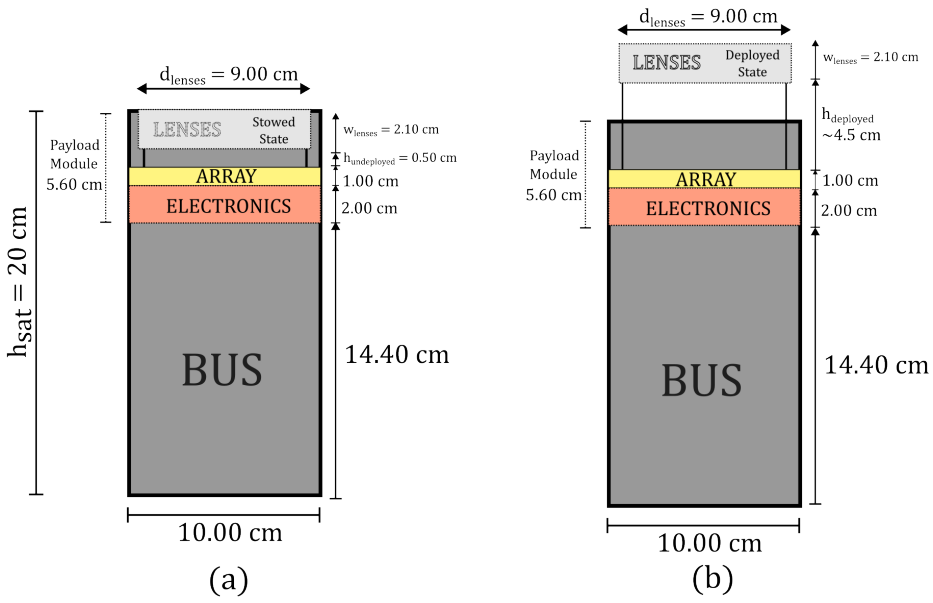

Figure 1. Mechanical deployment scheme for the PAFL antenna payload. This scheme shows the volumetric savings made by deploying payload lens to desired focal length. (a) Diagram of the stowed state, showing the lens payload stowed within the 2U envelope. This will be CLOVER-Sat's state during launch. (b) Diagram of the deployed state. The antennas are linearly actuated out of the 2U envelope, ensuring a 0.5 focal distance over aperture diameter ratio. This will be CLOVER-Sat's state during operations in orbit.

System Design Overview/Mission

To streamline the technology demonstration, a receive-only antenna was chosen to undertake a basic Earth science mission utilizing the beam scanning capabilities in the K-band. Following consultations with scientists at NASA Goddard, it was determined that the PAFL could interface with a radiometer to measure the thermal noise of water, with the objective of detecting differences in this noise signature between water and land. Water was selected as an ideal target due to its emissivity, the ratio of the energy radiated compared to a perfect emitter (blackbody), being close to 1. The receiver will operate at 22GHz, aligning with water's vibration mode at this frequency. In low Earth orbit, the PAFL will conduct emissivity measurements along its orbital path, creating a heat map of the surface. Figure 2 shows a simulated LEO orbit for the CLOVER-Sat payload generated by IrishSat's PySOL program that is sufficient for building this map. Figure 3 details an overview of the proposed mission.

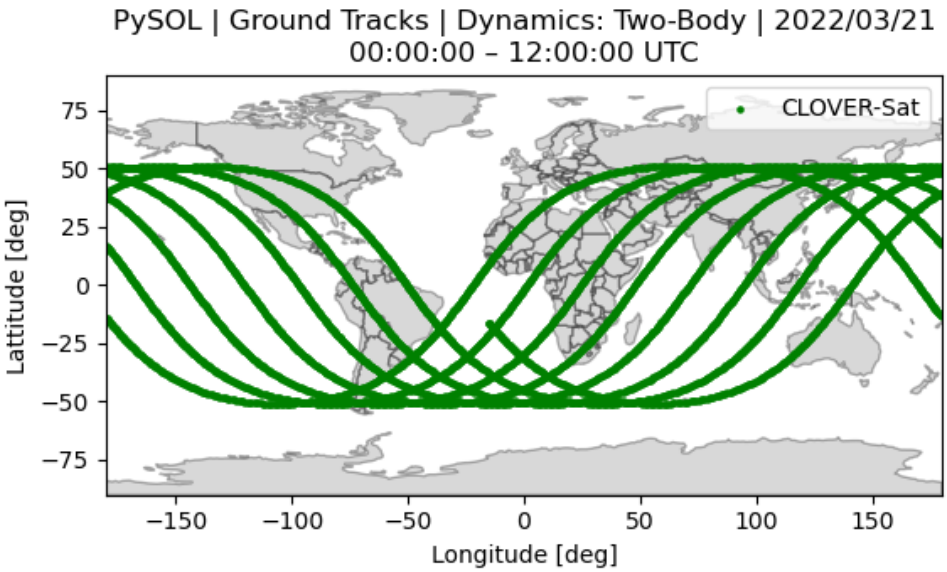

Figure 2. Target CLOVER-Sat orbit, propagated for 12 hours and visualized using IrishSat's custom orbital software, PySOL. The above figure depicts the orbit in (a) an Earth-centered inertial reference frame and (b) Earth-centered, Earth-fixed ground tracks, with the following orbital elements: eccentricity $e = 0.0001$, inclination $i = 51$ degrees, semimajor axis $a = 6,800$km, longitude of ascending node $\Omega = -30$ degrees, argument of periapsis $\omega = 80$ degrees, true anomaly $\nu = 121$ degrees. This is an example orbit that meets CLOVER-Sat's orbital requirements detailed in the CubeSat Mission Parameters.

Review of the Literature

Before undertaking this project, it was essential to develop an understanding of the scientific background regarding emissivity and noise, particularly as it pertains to the radiometer. Two distinct textbooks, "Radio Astronomy" by John Kraus and "Microwave Engineering" by David Kraus, served as references to delve deeper into black-body radiation, thermal electromagnetic radiation, and the noise environment within which our receiver would operate. Understanding the noise environment is crucial because the signal itself is a form of noise, requiring comprehension of how to accurately interpret the correct noise signal to meet mission requirements.

"Radio Astronomy" provides insights into black-body radiation, defining a black body as an idealized non-reflective entity. Blackbody radiation establishes a reference point for specific temperatures and frequencies, against which the thermal electromagnetic radiation of other substances can be measured, as elucidated by Kraus through Planck's radiation law. The measurement of the ratio of radiation from an object of interest to the radiation of a black body under defined physical conditions is known as emissivity. Additionally, the book outlines brightness curves, representing thermal electromagnetic radiation, with maximums occurring at different frequencies [2].

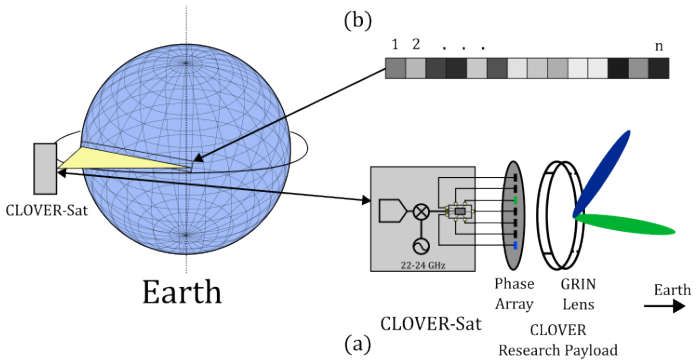

Figure 3. CLOVER-Sat mission concept, depicting CLOVER-Sat in LEO performing measurements by electronically scanning across one dimension. (a) The payload consists of a phased array fed gradient index lens antenna (b) The data received via 1D electronic beam-scanning will be an array of noise power amplitudes, i.e. an array of pixels.

Pozar's work offers radiometer-specific information on radiation and noise. The primary objective was to design a system capable of reading the thermal electromagnetic radiation of Earth's atmosphere from Low Earth Orbit (LEO). Antennas receive signals from a complex array of sources, both from the main lobe and side lobes, making it challenging to discern the desired signal, particularly if it has a low magnitude. Regarding thermal noise, Pozar provides equations describing the relationship between background noise temperature, antenna noise temperature, physical temperature, and other values contributing to the overall system noise temperature. This information proved invaluable in establishing design requirements for the radiometer [3]. Pozar also supplies essential information about the atmospheric background noise temperature at different frequencies, aiding in the selection of the design frequency. To measure the emissivity of water, the optimal frequency in the millimeter wavelength range is centered at 22 GHz, aligning with the vibration mode of water at this frequency, causing a spike in background noise temperature as illustrated in Figure 4.

By reading the noise temperature at 22 GHz, it becomes feasible to observe a noticeable distinction between bodies of water, attributed to variations in humidity levels, and measurements taken over land with lower humidity levels. This literature review facilitated the precise definition of specific system constraints and established a foundational knowledge base for constructing an emissivity map along CLOVER-Sat's orbital path.

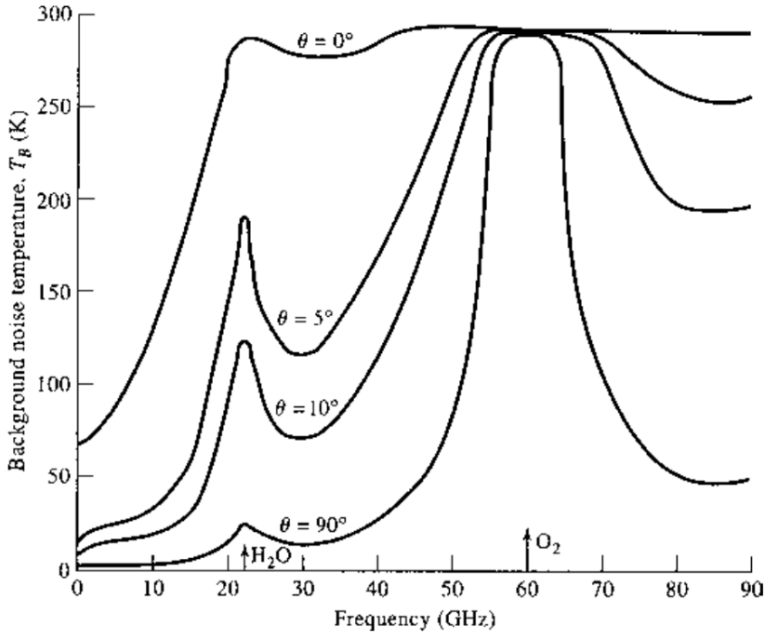

Figure 4. Background noise temperature of sky vs frequency. θ is elevation angle measured from horizon. Sourced from [insert here]

Designing the Circuit and Picking Parts

A radiometer is a device that measures the power of electromagnetic radiation at a specific wavelength. To construct one, electromagnetic signals from the environment are amplified and then demodulated into analog I and Q signal components, converting it to a digital bit stream that expresses the amount of electromagnetic energy present at its frequency. Several key components are essential in the design, including low noise amplifiers (LNA), a beamformer integrated circuit (BFIC), an I/Q demodulator, an analog-to-digital converter (ADC), and a microcontroller unit (MCU). Additionally, the I/Q demodulator requires an external linear oscillator (LO) and phase-locked loop (PLL) to function properly. Due to the extremely small temperature noise signals, designing the radiometer poses challenging considerations. Some specific design considerations for this radiometer that presented these challenges include:

1. The radiometer must have an extremely small effective noise figure.
2. The radiometer must have high overall gain so the signal can be converted from analog to digital form.
3. The radiometer components must all operate within the 22 GHz range, the frequency of interest for this research project.
4. The radiometer must account for changes in the overall gain of the circuit as temperature and other factors change over time to ensure reliable data readings.
5. All radiometer components must be space hardened and capable of withstanding the harsh environment in Low Earth Orbit (LEO).

Considering these design requirements, the radiometer's design commenced. Initially, the determination of how many array elements would be included in the 1D array of the PAFL antenna configuration was made, based on the sizing constraints of the 9cm diameter lens (a constraint imposed by satellite bus sizing). Settling on 12 elements, it was then established that 12 low noise amplifiers (LNAs) (one for each element) and a beamformer integrated circuit (BFIC) with at least 12 channels were necessary. The BFIC combines the incoming signals into one analog output, connected to the I/Q demodulator. After down-conversion from 22 GHz and demodulation into the signals' in-phase and quadrature components, these two components are sent to an analog-to-digital converter (ADC) for digitization. Subsequently, this digital signal is processed by the microcontroller. The microcontroller not only receives the digital signals but also manages the configuration and control of the LO, PLL, and BFIC for proper signal processing. The complete design, including part selections, can be found in Figure 5.

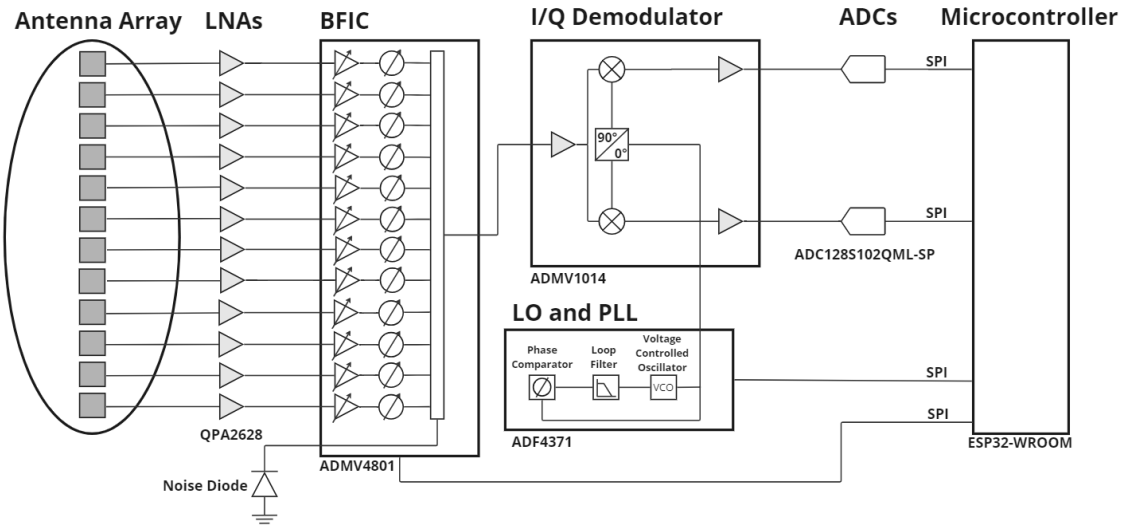

Figure 5. Block diagram showing the main electronic components that makeup the phased array fed lens payload. Each antenna element is in series with a low noise amplifier (LNA) that connects to the beamforming integrated circuit (BFIC). The resultant RF signals pass through a demodulator that interfaces with a analog digital converter (ADC) before being processed by a microcontroller.

Overview of PAFL Antenna and Radiometer Function

To facilitate beam scanning, a particle swarm algorithm computes optimal complex weights for each antenna, adjusting both the magnitude and phase of each element. This process is facilitated by an SPI communication protocol between the microcontroller and the beamformer IC. The outcome is a superimposed beam at an arbitrary angle capable of receiving a thermal noise signal. On the high end for a temperature of

276K, an expected -91dB signal is anticipated (Eq. 4).

Initially, a low noise amplifier (LNA) is employed in a gain cascade to apply high gain to the signal while introducing minimal circuit noise. This decision is pivotal due to the faint nature of the target signal. The desired specifications of a low power, low noise figure LNA within the required frequency range proved challenging to find. The lowest figure LNA meeting the frequency requirements was 1.4, which was deemed acceptable following subsequent noise calculations.

Subsequently, the beamformer IC provides further gain to the signal, creating a superimposed beam that minimizes the effect of slide and grading lobes, allowing the main lobe to detect most of the signal at the desired scanning angle. This stage also incorporates a noise diode connected to a channel of the BFIC, aiding in accurate measurements using comparative calibration techniques. The noise diode assists in tracking how circuit noise and circuit gain change with temperature and other factors. Since noise affects both the desired signals and the diode equally, it can be used to cancel out added noise in the circuit. By connecting and monitoring a noise diode close to the beginning of the cascade, adjustments in gain levels can be made over time when collecting data.

The signal from each of the 12 antenna elements is combined into a single RF transmission to the I/Q Demodulator. The I/Q Demodulator takes the signal from the BFIC and down-converts it from 22 GHz for processing by the analog-to-digital converters (ADCs), separating the signal into its I and Q components. The demodulator requires an external LO and PLL, configured via an SPI connection from the microcontroller to function properly, as shown in Figure 1. The radiometer is interfaced with the microcontroller by two ADCs with an SPI connection. The ADCs compare the input voltage from the power supply of 3.3V to the incoming signal. Its dynamic range, specified by the number of bits and the maximum input signal of 3.3V, determines its "observation window" of signals the radiometer is capable of detecting [4]. This information is converted into a binary format by comparing signal magnitude via a multiplexer (mux).

Calculations

The following calculations were used to justify this project's feasibility by quantifying the expected noise power that the radiometer is capable of characterizing for a range of temperature values as well as the estimated pixel size/sampling time and overall power consumption.

Gain and Noise Figure Cascade:

$$T_b = \begin{bmatrix} 290 & 20 \end{bmatrix} \text{K}$$

$$T_B = 0.95 * T_b$$

$$G_{cass} = G_1 + G_2 + G_3 = 72\text{dB} \quad \text{where} \quad G_1 = 27 \quad G_2 = 28 \quad G_3 = 17 \tag{1}$$

$$F_{cass} = F_1 + \frac{F_2 - 1}{G_1} + \frac{F_3 - 1}{G_1 * G_2} \quad \text{where} \quad F_1 = 1.4 \quad F_2 = 3.16 \quad F_3 = 3.55 \tag{2}$$

$$NF = 10 * log(F_{cass}) = 1.7\text{dB} \tag{3}$$

Noise Power from Target Signal:

$$e \approx 1 \quad \textit{emissivity of water}$$

$$P_n = 10 * log(\frac{k * B * T_B}{1\text{mW}}) = \begin{bmatrix} -91.19 & -102.80 \end{bmatrix} \text{dBm} \quad \textit{Noise Power} \tag{4}$$

Bit Resolution:

$$P_f = P_n + G_{cass} = \begin{bmatrix} -19.19 & -30.80 \end{bmatrix} \text{ dBm} \quad \textit{Noise Power after Cascade} \tag{5}$$

$$n = 12 \quad \textit{Number of bits}$$

$$DR = 6.02 * n = 72.24\text{dB} \quad \textit{Dynamic Range} \tag{6}$$

$$V_{in} = 3.3\text{V} \quad R_{in} = 500\Omega \quad \textit{Input Voltage and Series Resistance of ADC}$$

$$P_{in} = \frac{V_{in}^2}{2 * R_{in}} * 1000\text{mW} \quad \textit{Max Power into ADC} \tag{7}$$

$$OW = \begin{bmatrix} 10 * log(P_{in}) & 10 * log(P_{in}) - DR \end{bmatrix} \text{dBm} = \begin{bmatrix} 10.37 & -61.87 \end{bmatrix} \text{dBm} \quad \textit{Observation Window} \tag{8}$$

Gain Estimations for Pixel Resolution:

$$f = 22\text{GHz} \quad \lambda = \frac{c}{f} * 1000\text{mm}$$

$$A = \pi r^2 \text{ mm}^2 \quad \textit{Aperture Size} \tag{9}$$

$$D_o = \frac{4\pi}{\lambda^2} * A \quad \textit{Directivity} \tag{10}$$

$$\eta = 0.5 \quad \textit{Aperture Efficiency} \quad e_{rad} = 1 \quad \textit{Radiation Efficiency} \tag{11}$$

$$D = \eta D_o = 215.26 \quad G = e_{rad} D = 215.26 \tag{12}$$

$$HPBW = \sqrt{\frac{32500}{D}} = 12.29 \text{ (deg)} \tag{13}$$

Determine Pixel Parameters:

$$alt = 500\text{km} \quad v_{ground} = 7.8\text{km/s}$$

$$r_{pix} = alt * \tan(\frac{HPBW}{2}) = 53.82\text{km} \quad \textit{Radius of each Pixel} \tag{14}$$

$$t_{samp} = \frac{r_{pix} * 2}{v_{ground}} = 13.8\text{s} \tag{15}$$

Power Calculations:

LNA: 100mW $*$ 12 = 1.2W

BFIC: 150mW $*$ 13 channels = 1.95W

I/Q DeMod: 1.5W

PLL w/ VCO: 0.264W

ADC: 2.3mW $*$ 2 = 0.046W

Total Power Consumption: 4.96W

Future Work

Calculations have demonstrated the successful design of a 22 GHz radiometer that is space-operable. Design requirements, including identifying an LNA with a low noise figure in the desired frequency range and a sufficiently large gain cascade to discern small thermal noise signals, have been met. However, several next steps must be addressed in the upcoming semester for this project.

It is crucial to verify the viability of operating at sub-optimal frequencies for the mission. Since there are limited suitable parts designed to function at 22 GHz, some components, including the BFIC and I/Q demodulator, may operate sub-optimally. The effects of this will need to be examined on the theoretical system performance.

Following a more extensive qualification of the system, construction and testing must occur to determine necessary adjustments to the idealized design. Calibration needs to be thoroughly investigated, and interference characterization from other sources, such as the sun, should be addressed. These steps are essential for refining and optimizing the radiometer's performance in preparation for its deployment in space.

References

[1] Wei Wang et al. “Beamforming Phased-Array-Fed Lenses With >0.5λ-Spaced Elements”. In: *IEEE Transactions on Antennas and Propagation* 71.3 (Mar. 2023). Conference Name: IEEE Transactions on Antennas and Propagation, pp. 2208–2223. ISSN: 1558-2221. DOI: 10.1109/TAP.2023.3240085.

[2] John Kraus. *Radio Astronomy 2nd Edition. McGraw-Hill.* 1950.

[3] David Pozar. *Microwave Engineering Fourth Edition. John Wiley & Sons, Inc.* 2011.

[4] James D. Broesch. “Chapter 3 - DSP System General Model”. In: *Digital Signal Processing*. Ed. by James D. Broesch. Instant Access. Burlington: Newnes, 2009, pp. 27–36. ISBN: 978-0-7506-8976-2. DOI: https://doi.org/10.1016/B978-0-7506-8976-2.00003-1. URL: https://www.sciencedirect.com/science/article/pii/B9780750689762000031.